AAPS PharmSciTech, Vol. 15, No. 3, June 2014 (© 2014)
DOI: 10.1208/s12249-014-0086-y

Research Article

Liposomal Oxymatrine in Hepatic Fibrosis Treatment: Formulation, *In Vitro* and *In Vivo* Assessment

Shujuan Zhang,[1] Jun Wu,[2] Hua Wang,[3] Tiechuang Wang,[1] Lina Jin,[1] Dandan Shu,[1] Weiguang Shan,[1] and Subin Xiong[1,4]

Received 15 August 2013; accepted 17 January 2014; published online 12 February 2014

Abstract. The aim was to develop a liposomal oxymatrine conjugating D-alpha tocopheryl polyethylene glycol 1000 succinate (OMT-LIP) for enhanced therapeutics of hepatic fibrosis. OMT-LIP was prepared using the remote loading method. The influences of formulation compositions on the encapsulation efficiency of OMT-LIP were investigated. Mean particle size, zeta potential, morphology, *in vitro* release, fibrotic liver targeting, and therapeutics of OMT-LIP were thoroughly assessed. The intraliposomal buffer composition and concentration, extraliposomal phase composition and pH, types of phospholipid, lipid molar ratio composition, and theoretical drug loading are crucial factors to entrap OMT into liposomes. The optimum OMT-LIP presented spherically unilamellar microstructures with entrapment efficiency of 79.7±3.9%, mean particle size of 121.6±52.9 nm, and zeta potential of −5.87 mV. OMT-LIP significantly increased the accumulation of OMT in the fibrotic liver with an 11.5-fold greater AUC than OMT solution in the dimethylnitrosamine (DMN)-induced hepatic fibrosis animals. OMT-LIP could be a potential strategy to improve treatment outcomes for hepatic fibrosis, showing the protective effects to mice given CCl_4 and the enhanced therapeutics to mice with either DMN or CCl_4-induced hepatic fibrosis.

KEY WORDS: fibrotic liver targeting; hepatic fibrosis; liposomes; oxymatrine; therapeutics.

INTRODUCTION

Hepatic fibrosis is a pivotal and necessary stage during the development of chronic liver diseases to cirrhosis or hepatocellular carcinoma, which is also a cause of morbidity and mortality worldwide (1,2). Current investigations showed that hepatic fibrosis and cirrhosis at the early stage may be reversible (3). Therefore, the effective treatment for hepatic fibrosis is critical to avoid the deterioration of chronic liver diseases.

Hepatic fibrosis is initiated by the comprehensive actions of many cells, such as active Kupffer cells, sinusoidal endothelial cells, hepatic stellate cells (HSCs), and infiltrating inflammatory cells, when hepatocytes are being damaged by hepatitis B or C viral infection, drug or alcoholic toxicity, and cholestasis. The deposition of large amounts of extracellular matrix (ECM) components, such as collagens, is a crucial marker of fibrosis (4–6). The collagens in the space of Disse will accentuate the narrowing and distortion of the sinusoidal lumen and the formation of fibrotic septa, which would restrict the microvascular blood flow and result in hypoxia. Then, the angiogenesis is stimulated by the hypoxia-induced upregulation of vascular endothelial growth factor (VEGF), Ang, and receptors in HSCs (7). The distorted vessels, the same as the solid tumor's, with the enhanced permeability and retention (EPR) effect (8), could contribute to the targeted delivery to fibrotic liver.

Oxymatrine (OMT) is an active pharmaceutical ingredient from the dried roots of traditional Chinese medicines named *Sophora flavescens* Ait (Kushen) or *Sophora alopecuroides* (Kudouzi), with anti-fibrosis effects by inhibiting the activation and proliferation of HSCs, and synthesis of ECM components, reducing the production of pro-inflammatory cytokines (TNF-α, IL-1, or IL-6) and oxygen radicals, and downregulating the gene expression of a pro-fibrotic cytokine TGF-β1 (9,10). The anti-fibrosis therapeutics depends on the dose and exposure time of OMT. However, OMT is distributed widely in the tissues and eliminated rapidly after intravenous injection (11).

Targeted delivery of OMT to hepatic fibrosis tissues is crucial to improve the therapeutic efficacy. Liposome is a biocompatible nanocarrier for liver-targeted delivery (12). D-Alpha tocopheryl polyethylene glycol 1000 succinate (TPGS) is a water-soluble vitamin E derivate with PEG chain. Our previous studies showed that TPGS improved the physical stability and increased the encapsulation efficiency of poorly water-soluble emodin into liposomes (13). Evidence suggested that antioxidant agents, such as vitamin E, have been used to

[1] College of Pharmaceutical Sciences, Zhejiang University of Technology, 18 Chaowang Road, Hangzhou, 310032, People's Republic of China.
[2] College of Pharmacy, University of South Carolina, Greenville, South Carolina 29605, USA.
[3] Center of Analysis and Measurement, Zhejiang University, 268 Kaixuan Road, Hangzhou, 310029, People's Republic of China.
[4] To whom correspondence should be addressed. (e-mail: xiongsb@zjut.edu.cn)

prevent and treat chronic liver diseases, such as hepatic fibrosis (14–16). It has also been demonstrated that TPGS inhibited the intercellular distribution of fibronectin and the proliferation of human skin fibroblasts (17). We hypothesized that TPGS could work as a pegylated agent to formulate OMT liposomes and show synergistic therapeutics to hepatic fibrosis.

Dimethylnitrosamine (DMN) and carbon tetrachloride (CCl_4) have been widely used to induce murine liver fibrosis models (18,19). In this study, a novel liposomal OMT conjugating TPGS was formulated and OMT was loaded into liposomes using a remote loading method. Characterization of OMT-LIP was investigated. Fibrotic liver targeting and therapeutics of OMT-LIP to the mice with hepatic fibrosis were also compared with OMT solution (OMT-SOL).

MATERIALS AND METHODS

Materials

Oxymatrine (99% purity) was purchased from Shanxi Sciphar Biotech., Co., Ltd (Shanxi, China). Egg phosphatidylcholine (EPC) and hydrogenated soy phosphatidylcholine (HSPC) were purchased from Avanti Polar Lipids, Inc. (Alabaster, AL). Soy phosphatidylcholine (SPC) and cholesterol (Chol) were purchased from Acros Organics (Fair Lawn, NJ). TPGS was kindly provided by Xinchang Pharmaceutical Company (Shaoxing, China). Extruder was purchased from Wuhan Huayao Biotech., Ltd (Wuhan, China). Acetonitrile (HPLC grade) was purchased from Tedia Co., Inc. (Fairfield, OH). All other reagents were of analytical grade.

Preparation of Liposomes

Liposomes were prepared by thin film hydration, followed by polycarbonate membrane extrusion. OMT was loaded into liposomes using a remote loading method. Briefly, the lipids PC/Chol/TPGS were dissolved in chloroform and dried to thin film with rotary evaporation under reduced pressure. The lipid film was hydrated with buffer (pH 4.0). The generated multilamellar liposomes were extruded five times through a 200-nm pore-sized polycarbonate membrane (Whatman, Maidstone, Kent, UK) under nitrogen to produce unilamellar vesicles. The buffer (pH 4.0) outside liposomes was exchanged with tangential flow diafiltration using a Millipore Pellicon XL cartridge with a MWCO of 30 kDa; the empty liposomes containing the final lipid concentration of 10 mg/ml were collected. OMT stock solution (20 mg/ml) was mixed with empty liposomes and the mixture incubated for 15 min at 37°C with occasional shaking.

Parameters affecting the encapsulation efficiency of OMT-LIP, such as intraliposomal acidic buffer, extraliposomal continuous phase, lipid composition, and theoretical drug loading, were investigated.

Characteristics of Liposomes

Free and liposomal OMT were separated with size exclusion chromatography on a Sephadex G-50 column. Liposomal OMT were lysed by 1.0% Triton X-100 and OMT was assayed with HPLC, as described below. Encapsulation efficiency was calculated according to equation $\mathrm{EE} = \frac{W_{liposomal-OMT}}{W_{free-OMT}+W_{liposomal-OMT}} \times 100\%$.

Particle size and distribution and the zeta potential of liposomes were determined with dynamic light scattering (Delsa Nano; Santa Barbara, CA). The ultrastructure of OMT-LIP was investigated using transmission electron micrography (JEM-1400; Jeol, Japan) after negative staining with sodium phosphotungstate solution (2%, *w*/*v*).

In vitro release study was measured using the dialysis method. OMT-LIP was placed in the dialysis bag, immersed in PBS (pH 7.4) or acetate buffer (pH 5.0), and then incubated in a water bath (37°C, 75 rpm). At the preset time intervals, the concentrations of OMT in the media were determined with the HPLC method, as described below. All experiments were repeated three times and the results presented as the mean±SD (n=3).

Animals

The animal study was performed with the approval of the Institutional Animal Ethics Committee of Zhejiang University of Technology (2009001, approval date 07 Jan 2009), and all the experiments were performed according to the guide for the Care and Use of Laboratory Animals.

Male ICR mice weighing 20–22 g were purchased from Shanghai Slac Laboratory Animal, Co., Ltd. All mice were fed and maintained under constant conditions at temperatures of 20–25°C and humidity 55±5%, with 12-h light and 12-h dark cycles. Water and food were accessible to mice *ad libitum*.

Animal Models of Hepatic Fibrosis

DMN was intraperitoneally injected to mice at a dose of 10 mg/kg for three consecutive days per week until week 4 to develop a DMN-induced hepatic fibrosis model. CCl_4 in corn oil (50:50, *v*/*v*) was orally administered to mice at a dose of 2 ml/kg two times per week for 10 weeks to develop a CCl_4-induced hepatic fibrosis model.

Hepatic fibrosis animal models were successfully established by the liver histopathological evaluation.

Fibrotic Liver Targeting

Mice with DMN-induced hepatic fibrosis were randomly divided into two groups (24 mice in each group): OMT-LIP and OMT-SOL. A single dose of OMT 10 mg/kg was intravenously injected. At 5, 15, 30, 60, 120, 240, 480, and 720 min after administration, animals (three per time point) were killed. Blood was collected in tubes with heparin from mouse orbital sinus and plasma was obtained after centrifugation at 3,500 rpm for 5 min. The liver was removed, washed by cold saline, blotted with filter paper, and weighed.

Sample Preparation

The liver (0.5 g) was homogenized in saline (1.0 ml). Plasma or liver homogenate (300 μl) was placed in 5-ml polyethylene tubes. Methanol (100 μl) and dichloromethane (3 ml) were added, mixed for 2 min by vortex, and then centrifuged at 5,000 rpm for 5 min. The organic phase was transferred to a fresh 5-ml polythene tube and dried by air stream at 40°C. The

residue was reconstituted in 50 μl mobile phase and centrifuged at 10,000 rpm for 10 min before determination. A sample (15 μl) was injected into HPLC.

Chromatography

The samples were analyzed at ambient temperature utilizing a 4.6×250-mm ODS column (5 μm, Elite, Dalian, China), preceded by a 5-mm guard column packed with ODS. The mobile phase was a mixture of 0.1% phosphoric acid solution (pH 3.0, containing 0.1% triethylamine) and acetonitrile (92:8) at a flow rate of 0.8 ml/min.

The HPLC instrument consisted of a LC-10ADT pump (Shimadzu, Kyoto, Japan) and an SPD-10A UV/Vis detector at a wavelength of 220 nm. The chromatographic data were managed using an N2000 software (Zhejiang University, Zhejiang, China). Overall, the absolute extraction efficiencies were above 73% in mouse plasma and above 63% in the mouse liver. The relative recoveries were above 98% in mouse plasma and 95% in the mouse liver.

Therapeutic Efficacy Against DMN or CCl_4-Induced Hepatic Fibrosis

Mice with DMN or CCl_4-induced hepatic fibrosis were randomized to four groups, each group with ten mice. OMT-LIP and OMT-SOL were intravenously injected at a single dose of 10 mg/kg every other day, with a total dose of 100 mg/kg for 20 days, respectively. The control group and empty liposomes (Empty-LIP) were intravenously given (0.2 ml per mouse) with the same regimen.

At the end of treatments, animals were killed and liver specimens were collected and fixed in 10% formalin. The liver tissues were embedded in paraffin, sliced into 4-μm-thick sections, and stained with hematoxylin–eosin and Masson's trichrome, respectively. A numerical scoring system for assessing the histological fibrosis was used to evaluate the therapeutic efficacy (20). Briefly, fibrosis was divided into four stages: no fibrosis (stage 0), enlarged, fibrous portal tracts (stage 1), periportal or portal–portal septa but intact architecture (stage 2), fibrosis with architectural distortion (stage 3), and probable or definite cirrhosis (stage 4).

Prophylactic Efficacy Against CCl_4-Induced Hepatic Fibrosis

Mice were randomly divided into five groups, such as healthy group and four prophylactic groups, with ten mice for each group. CCl_4 in corn oil (50:50, *v*/*v*) was orally administered at a dose of 2 ml/kg two times per week until week 10. Starting on the first day of CCl_4 administration, OMT-LIP and OMT-SOL at a single dose of 10 mg/kg were intravenously injected every 3 days, with a total dose of 240 mg/kg over 10 weeks, respectively. The control group and Empty-LIP were intravenously given (0.2 ml per mouse) with the same regimen. At the end of the tenth week, liver histology was assessed as above.

Statistical Analysis

Data were reported as the mean±SD. *T* tests were performed for two group comparisons; one-way ANOVA tests were used for data with more than two groups. Based on ANOVA test results, post hoc Tukey's tests were applied for multiple comparisons between groups. The statistical significance level was set at $P<0.05$.

RESULTS AND DISCUSSION

Preparation of Liposomes

OMT is a weakly basic drug. It has been reported that OMT was loaded into PC/Chol/DCP liposomes with entrapment efficiency of 60.17% using a reversed-phase evaporation technique (21), or into PC/Chol liposomes with entrapment efficiency of 50% with the remote loading method (22). In our study, we found that liposomes composed of SPC/Chol or EPC/Chol aggregated during storage at 4°C for several hours. TPGS is a surfactant (HLB 13) with the hydrophobic chain of vitamin E and hydrophilic chain of PEG. Thus, a novel OMT liposomal formulation composed of EPC/Chol/TPGS was thoroughly investigated based on the pH gradient remote loading method.

SPC was used as the phospholipid to explore the effects of various pH gradients on the encapsulation efficiency of liposomes. Although doxorubicin and other basic drugs, such as daunorubicin, mitoxantrone, and chloroquine, were loaded into liposomes under the pH gradients induced by $(NH_4)_2SO_4$ (23–25), the lowest incorporation of OMT (17.9±2.2%) was obtained. Citrate, such as NH_3-citric acid or citrate buffer, is another pH gradient used in the remote loading process for weakly basic drug (23,26), which significantly improved the entrapment of OMT (57.4±1.5% and 62.7±3.1%) in comparison with $(NH_4)_2SO_4$ ($P<0.05$), while no significant difference between NH_3-citric acid and citrate buffer was observed ($P>0.05$), as shown in Fig. 1a. Except for the transmembrane pH gradient, ion gradient, such as phosphate, has also been reported to load doxorubicin into liposomes and allow the drug to be released from liposomes faster than that of $(NH_4)_2SO_4$ *in vitro* (26). However, we found that the loading efficiency of OMT into liposomes was only 24.3±2.7% under NH_3/H_3PO_4–induced ion gradient. These data suggested that the citrate buffer not only provided the pH gradient to pull the unionized OMT into liposomes but also allowed the unionized OMT to dissociate in the intraliposomal acidic condition and form the complex with ionized OMT.

The relationship between the concentrations of citrate buffer and the encapsulation efficiency of OMT-LIP was illustrated in Fig. 1b. Increased concentration of citrate buffer from 50 to 300 mM was necessary to withdraw the hydration shell of amphiphilic OMT and make OMT precipitate in liposomes to achieve an encapsulation efficiency of 62.7±3.1% at 300 mM ($P<0.05$).

The composition and pH value of the continuous phase outside liposomes were also critical to load OMT into liposomes based on the citrate buffer-driven pH gradient. When the pH values outside liposomes are similar, such as saline and sucrose (10%), due to the stronger interaction of OMT with extraliposomal Cl^- than the intraliposomal citrate, which inhibited OMT loading into liposomes, a significantly lower incorporation efficiency by saline results ($P<0.05$), as presented in Fig. 1c. When the continuous phase was an isotonic PBS solution and the pH levels changed from 7.4 to

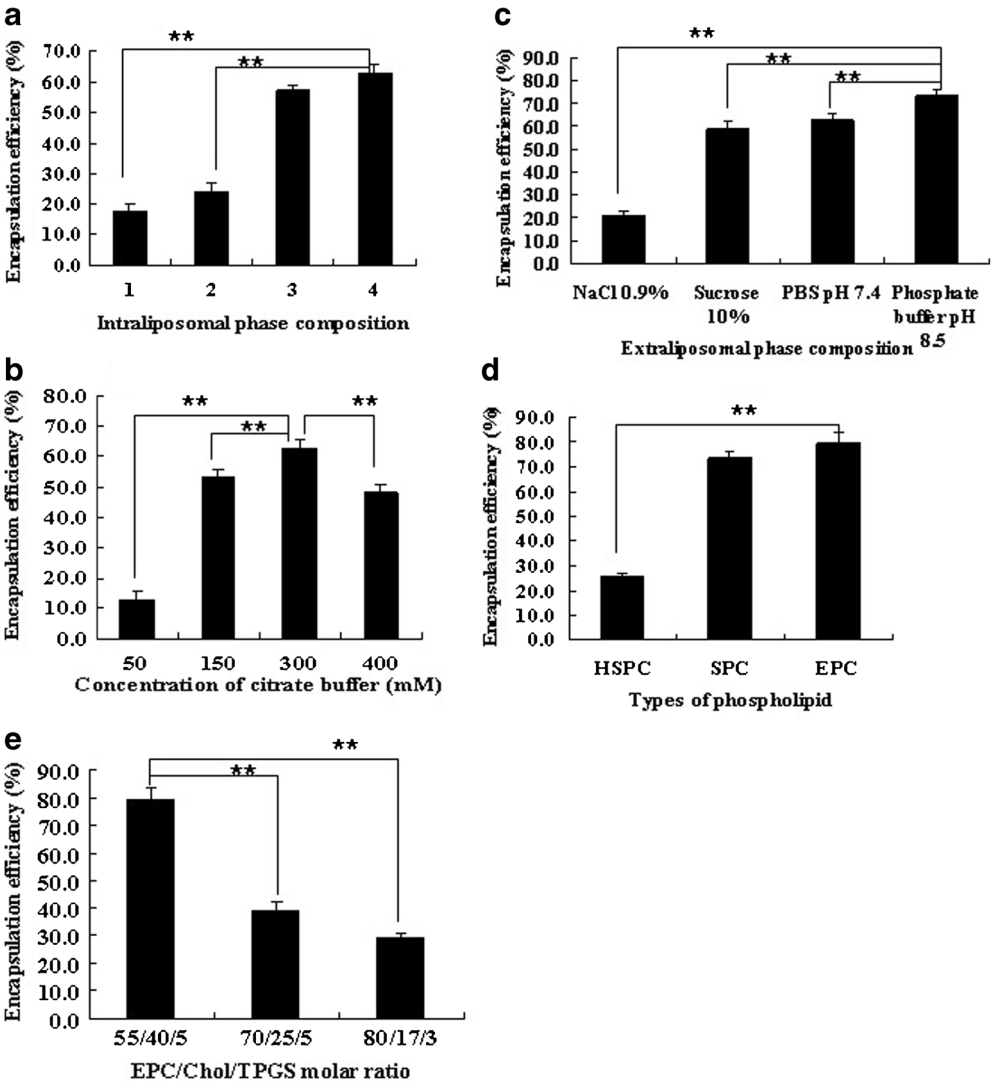

Fig. 1. Factors influencing the encapsulation efficiency of OMT-LIP using the remote loading method. **a** Intraliposomal phase composition with a concentration of 300 mM, pH 4.0 (*1*, $(NH_4)_2SO_4$; *2*, NH_3–H_3PO_4; *3*, NH_3-citric buffer; *4*, citrate buffer). **b** Intraliposomal citrate buffer concentrations. **c** Extraliposomal phase compositions. **d** Types of phospholipid. **e** EPC/Chol/TPGS molar ratio. $^{**}P<0.05$. *Error bars* refer to standard deviations ($n=3$)

8.5, the entrapment efficiency was raised from 62.7±3.1% to 67.8±3.0%. Furthermore, phosphate buffer (pH 8.5) was used to induce the pH gradient and the OMT loading efficiency was 73.3±2.9% ($P<0.05$).

The effects of lipid composition on the encapsulation efficiency of liposomes have been widely discussed previously (23), which were also observed in the OMT-LIP, as displayed in Fig. 1d. HSPC is the hydrogenated product of unsaturated SPC, with much better stability than SPC, and has been used in commercial liposomes. It is worth noting that phospholipids with unsaturated fatty acids, such as SPC (73.3±2.9%) and EPC (79.7±3.9%), can entrap much more OMT into liposomes than HSPC without C=C bonds ($P<0.05$). It is well known that HSPC liposomes show a more rigid structure than SPC or EPC liposomes. OMT is a molecule with four chiral carbons and two hydrogen bond acceptors. Thus, the fluidity of SPC or EPC liposomes allowed the transmembrane movement of OMT by its rotating motion and intermolecular

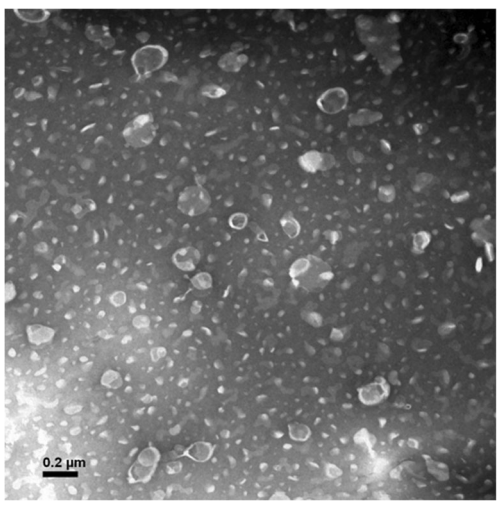

Fig. 2. TEM image of OMT-LIP by negative staining with sodium phosphotungstate solution (×50,000)

Table I. Encapsulation Efficiency and Particle Size of OMT-LIP During Storage at 4°C

Time (days)	EE (%)	Particle size (nm)
0	80.1±3.7	125.4±43.5
10	76.1±3.9	121.8±45.5
30	72.4±0.7	126.7±46.8

Data were shown as the mean±SD (n=3)

hydrogen bond, which resulted in a notably higher encapsulation efficiency than that of HSPC. Although there was no significant difference of entrapment efficiency between SPC and EPC liposomes (P>0.05), EPC liposomes demostrated much more stability than SPC.

The effects of the molar ratios of EPC/Chol/TPGS and theoretical drug loadings on the encapsulation efficiency of liposomes were also studied. As the lipid compositions of EPC/Chol/TPGS ranged from 55:40:5 to 80:17:3 (molar ratio), the encapsulation efficiency decreased significantly (P<0.05), as shown in Fig. 1e. When the theoretical drug loading was 10% (w/v), the encapsulation efficiency was 79.7±3.9% (P<0.05).

Put together, the OMT-LIP composed of EPC/Chol/TPGS (molar ratio, 55:40:5) was formulated by the driven actions of pH or ion gradient and intraliposomal precipitation of the drug–reverse ion complex, which showed a much higher encapsulation efficiency than those published (21,22).

Characterization of Liposomes

The unilamellarly spherical microstructure of OMT-LIP was observed with TEM using negative staining (Fig. 2). These liposomes contained OMT 1.0 mg/ml and phospholipid 10.0 mg/ml with a particle size of 121.6±52.9 nm and zeta potential of −5.87 mV. The entrapment efficiency of OMT was 79.7±3.9%.

To explore the stability of OMT-LIP at 4°C, the encapsulation efficiency and particle size were tested during storage for 1 month. The data showed that the encapsulation efficiency was decreased by 5.0% at 4°C after 10 days and 9.6% after 30 days. Particle size was similar during the storage, as listed in Table I. These results suggest that although TPGS improves the physical stability of empty EPC/Chol liposomes, OMT-LIP should be lyophilized as powders for long-term stability.

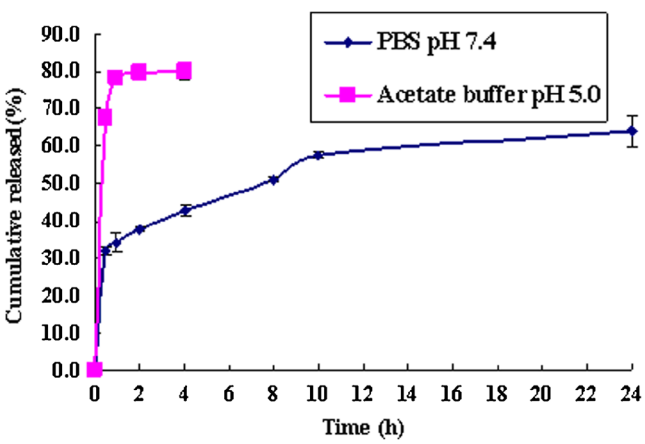

Fig. 3. *In vitro* release of OMT-LIP in PBS (pH 7.4) and acetate buffer (pH 5.0) media. *Error bars* refer to standard deviations (n=3)

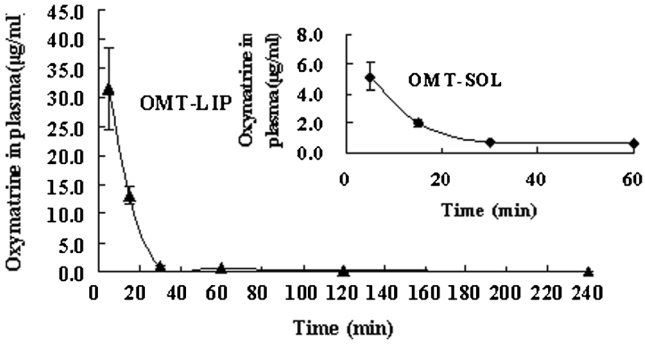

Fig. 4. OMT plasma concentration versus time after intravenous injection of OMT-LIP to hepatic fibrosis mice in comparison with OMT-SOL. *Error bars* refer to standard deviations (n=3)

To examine the stability and drug release properties of OMT-LIP, an *in vitro* release study was carried out in PBS (pH 7.4) and acetate buffer (pH 5.0), respectively. The results showed that the burst release was 34.2±2.5% in PBS (pH 7.4) after 1 h and the cumulative release was 63.9±4.4% after 24 h. The *in vitro* release of OMT-LIP in acetate buffer (pH 5.0) was much faster than that in PBS (pH 7.4), with 78.1±1.5% of OMT being released after 1 h (Fig. 3). The results of *in vitro* release suggest that OMT-LIP could be delivered to the fibrotic liver and quickly released in the acidic endosomes after endocytosis by the targeted cells.

Fibrotic Liver Targeting

The angiogenesis, stimulated by the hypoxia-induced up-regulation of VEGF, Ang, and their receptors in HSCs, is an important feature for the fibrotic liver (7,27). It could serve as

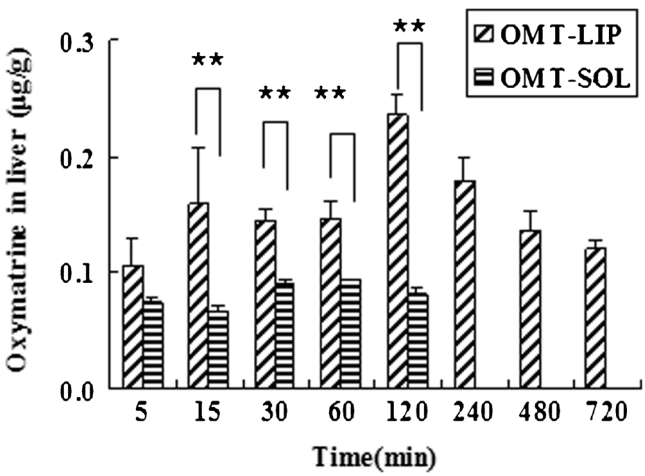

Fig. 5. Biodistribution of OMT-LIP in the fibrotic liver post-intravenous injection in comparison with OMT-SOL. **P<0.05. At 240, 480, and 720 min, the OMT levels were below the detection limit in OMT-SOL. *Error bars* refer to standard deviations (n=3)

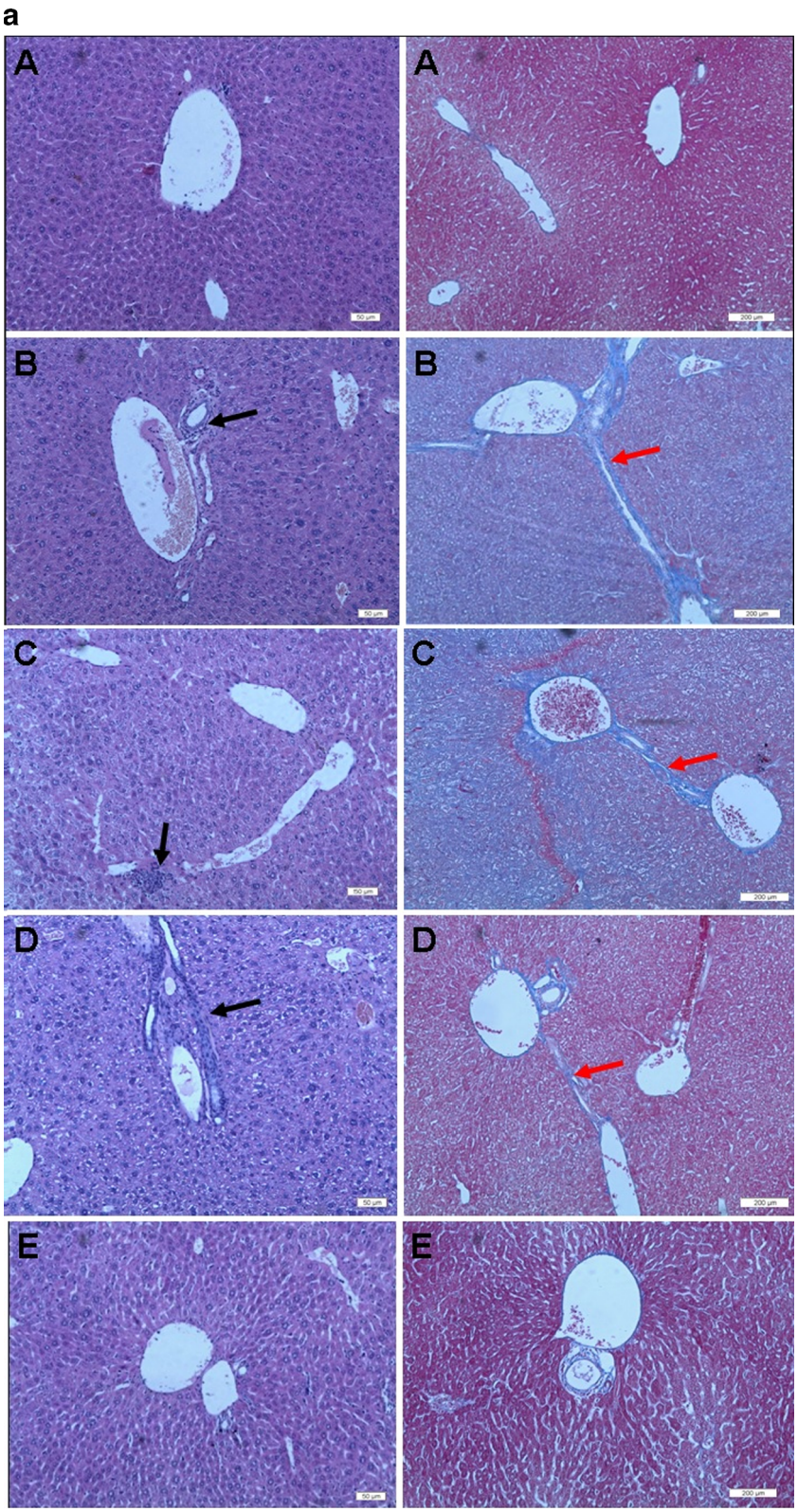

Fig. 6. Representative photographs of cross-sections of liver in mice with liver fibrosis induced by DMN (**a**) and in mice with liver fibrosis induced by CCl_4 (**b**) (*A*, healthy group; *B*, saline control group; *C*, empty liposome group; *D*, OMT-SOL group; *E*, OMT-LIP group). *Black arrow*, inflammatory cells; *white arrow*, necrotic hepatocytes; *blue arrow*, swollen hepatocytes; *yellow arrow*, fatty degeneration; *red arrow*, deposited collagens. *Left panel* Hematoxylin–eosin staining. *Bar*, 50 μm. *Right panel* Masson's trichrome staining. *Bar*, 200 μm

the delivery channels for nanocarrier targeting systems, similar to the EPR effect of solid tumor (8). Therefore, the plasma concentration versus time and liver targeting of OMT-LIP were carried out on the DMN-induced hepatic fibrosis animals. Due to the physical instability and low encapsulation efficiency of EPC/Chol liposomes without TPGS, we compared OMT-LIP and OMT-SOL in the animal study. Areas under concentration (AUC) were calculated by non-

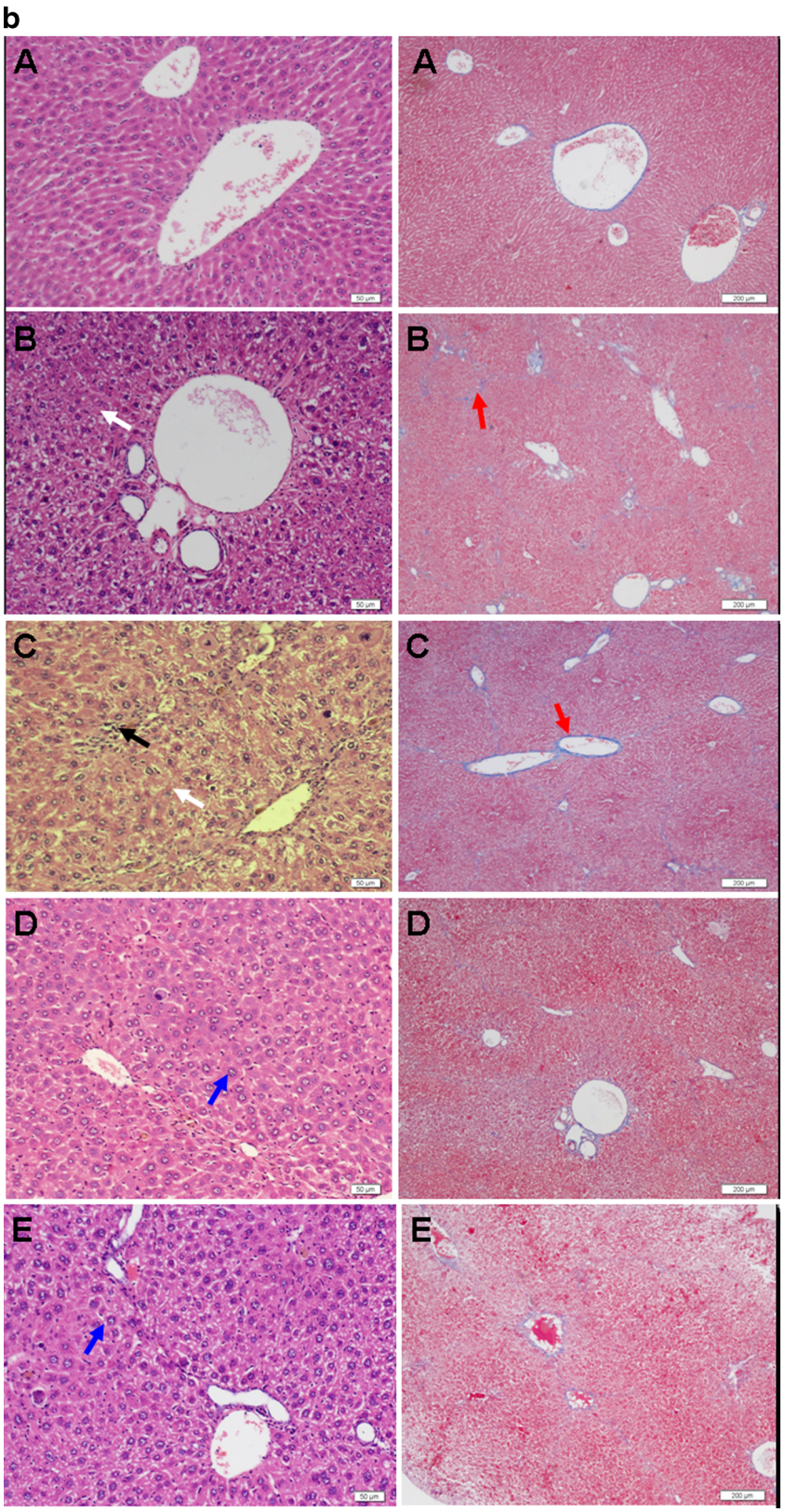

Fig. 6. (continued)

compartmental analysis using WinNonlin software (version 5.2, Pharsight Corp., USA).

Significantly higher OMT plasma concentrations of 31.46±6.91 μg/ml for hepatic fibrosis animals dosed with OMT-LIP in comparison with those OMT-SOL (5.11± 0.93 μg/ml, $P<0.05$) at 5 min and 13.16±1.53 μg/ml versus 2.02±0.24 μg/ml ($P<0.05$) at 15 min were detected. In addition, the plasma levels of OMT-LIP could be assayed until 240 min, while those of OMT-SOL cannot be detected at 120 min (Fig. 4). The $AUC_{0\rightarrow240\ min}$ of OMT-LIP was 5.4-fold that of OMT-SOL. These data indicate that EPC/Chol liposomes conjugating TPGS prolong the blood circulation time of OMT.

The biodistribution of OMT-LIP to the fibrotic liver was displayed in Fig. 5. Compared to OMT-SOL, significantly higher concentrations of OMT-LIP in fibrotic liver were detected from 15 min through 720 min ($P<0.05$). The OMT levels were under the detection limit at 240 min in the OMT-SOL. The $AUC_{0\rightarrow720\,min}$ of OMT-LIP showed an 11.5-fold increase in comparison with OMT-SOL. These indicate that OMT quickly distributes into the mice fibrotic livers from both solution and liposomes. Since soluble OMT in the aqueous

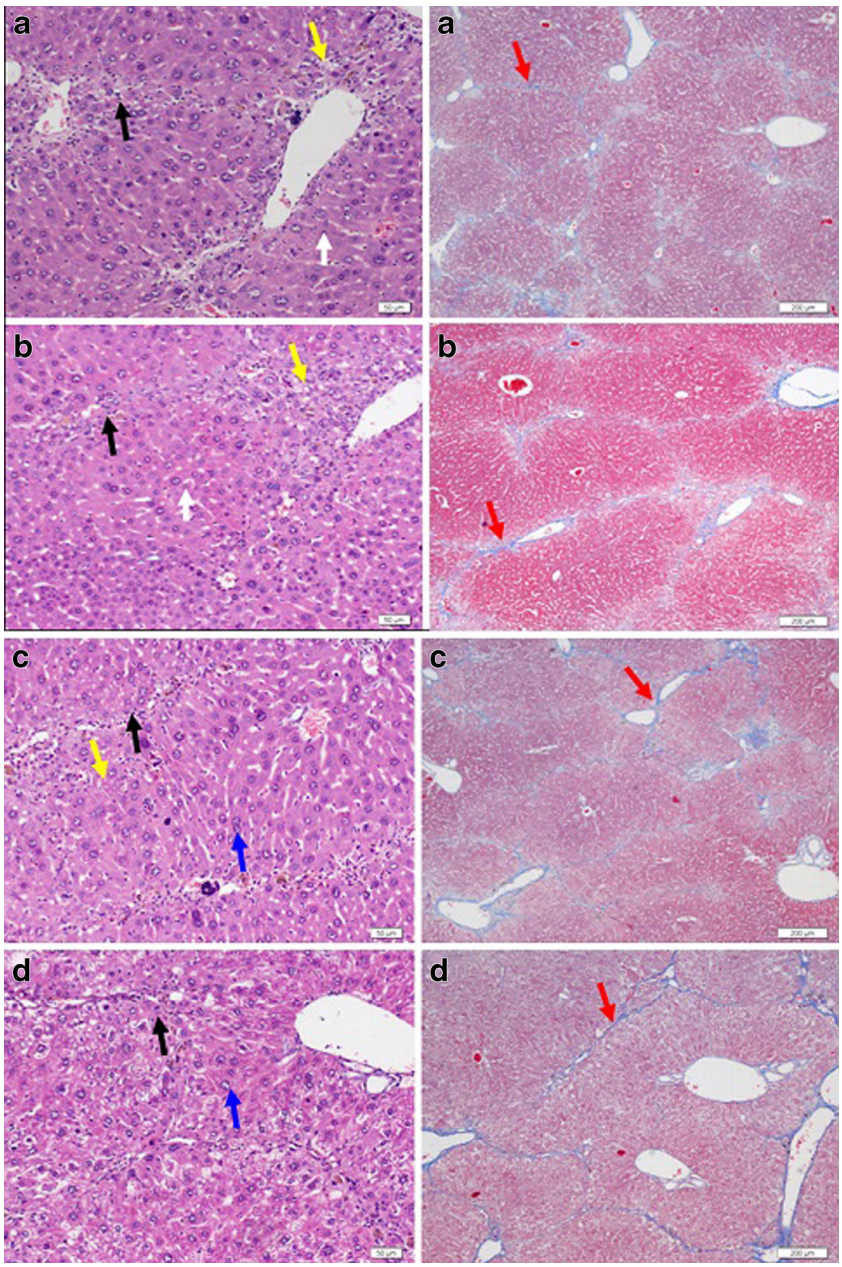

Fig. 7. Representative photographs of cross-sections of liver in the prophylactic study against liver fibrosis induced by CCl_4: saline control group (**a**), empty liposome group (**b**), OMT-SOL group (**c**), OMT-LIP group (**d**). *Black arrow*, inflammatory cells; *white arrow*, necrotic hepatocytes; *blue arrow*, swollen hepatocytes; *yellow arrow*, fatty degeneration; *red arrow*, deposited collagens. *Left panel* Hematoxylin–eosin staining. *Bar*, 50 μm. *Right panel* Masson's trichrome staining. *Bar*, 200 μm

solution is metabolized fast and eliminated rapidly from the body, EPC/Chol liposomes conjugating TPGS extend the accumulation of OMT in the interstitial liver tissues or endosomes of fibrotic cells, which works as the passively targeted delivery carrier for hepatic fibrosis treatment.

Therapeutic or Prophylactic Efficacy Against Hepatic Fibrosis

Although DMN and CCl_4-induced hepatic fibrosis models showed similar characteristics to human liver fibrosis, their different pathological characteristics have been reported previously (28). In our studies, the normal hepatocytes, clear and integrated architecture of hepatic lobules, the radially distributed hepatic plates, and no proliferation of connective tissues were seen in healthy mice. In the DMN-induced fibrotic animals, huge amounts of lymphomonocyte infiltration near the portal vein were clearly observed, the connective tissues built up, and the excessive extracellular matrix accumulated to form the fibrotic collagens around the central veins and sinusoids (Fig. 6a); in the CCl_4-induced fibrotic mice, hepatocyte necrosis, and pseudo-lobules by the deposited collagens were the major features (Fig. 6b).

Vitamin E inhibited the intercellular distribution of fibronectin and proliferation of human skin fibroblasts, which was also illustrated in the TPGS (17,29). In this study, we wanted to explore whether TPGS-tailored liposomes or TPGS would enhance the effects of OMT to fibrotic liver. The therapeutic efficacy of OMT-LIP and OMT-SOL against DMN or CCl_4-induced hepatic fibrosis was compared with liver histopathological assessment. The dosage regimen has been outlined in "MATERIALS AND METHODS."

Therapeutic Efficacy Against DMN-Induced Hepatic Fibrosis

The antifibrosis effects of OMT-LIP, OMT-SOL, Empty-LIP, and the control group were compared (Fig. 6a). In the OMT-SOL-treated group, the deposited collagens were partially reduced, which indicated that the degree of liver fibrosis was alleviated, while the infiltrated inflammatory cells and the thicker, even distorted or clogged sinusoid walls still existed. Surprisingly, the fibrotic septa dramatically diminished and the liver tissues were restored to almost normal in the OMT-LIP-treated group, while no clearly attenuated phenomena were observed in the Empty-LIP group.

Therapeutic Efficacy Against CCl_4-Induced Hepatic Fibrosis

The histopathological differences of CCl_4-induced hepatic fibrosis mice on the 20th day post-treatment were still observed (shown in Fig. 6b). Infiltrated inflammatory cells around the portal veins, large necrosis, and smaller amounts of hepatocytes can be seen in the images of the control and Empty-LIP groups stained by hematoxylin–eosin, while in the images of the OMT-SOL and OMT-LIP groups, only a few hepatocytes were swollen.

Various sizes of the pseudo-lobules were formed by the deposited collagens in the control and Empty-LIP groups. A larger size of pseudo-lobules in the OMT-SOL group was still seen in the images stained with Masson's trichrome. No pseudo-lobules were observed in the OMT-LIP group.

Prophylactic Efficacy Against CCl_4-Induced Hepatic Fibrosis

The prophylactic effects of OMT-LIP, OMT-SOL, and empty liposomes were compared by intravenously administering a single dose of 10 mg/kg every 3 days continuously for 10 weeks (Fig. 7). In comparison with the therapeutics, infiltrated inflammatory cells around the portal veins, large necrotic hepatocytes, formation of vacuoles by fatty degeneration, and smaller amounts of hepatocytes in the control and Empty-LIP groups were observed, while relative uniform, except for a few swollen, hepatocytes in OMT-SOL and OMT-LIP were also observed in the hematoxylin/eosin-stained images. The results suggest that OMT shows protection to hepatocytes.

In the images stained with Masson's trichrome, large amounts of the pseudo-lobules formed by the deposited collagens in the groups of control, Empty-LIP, and OMT-SOL and a small quantity of pseudo-lobules in the OMT-LIP group were seen.

The above results suggest that TPGS-tailored liposome is appropriate for a passively targeted delivery of OMT to the fibrotic liver. However, due to the dose limit of TPGS in the liposomal OMT, the synergistic effects of TPGS need further study.

CONCLUSIONS

The novel TPGS-tailored liposomal OMT formulation showed desirable physical stability and properties, with high loading efficiency, appropriate mean particle size, and zeta potential for liver targeting. OMT-LIP increased drug accumulation in the fibrotic liver, enhanced therapeutic efficacy against DMN or CCl_4-induced hepatic fibrosis, and showed protective effects against CCl_4 inducing fibrosis in comparison with OMT-SOL.

ACKNOWLEDGMENTS

This work was supported by the Chinese Traditional Medicine Bureau of Zhejiang Province grant (2006C154), Science Technology Department of Zhejiang Province grant (2009F70017), and the analytical funding from Zhejiang University of Technology. The authors are grateful to Dr. Ximei Wu of the Zhejiang University School of Medicine for his technical help in liver histological sections.

REFERENCES

1. Iavarone M, Colombo M. HBV-related HCC, clinical issues and therapy. Dig Liver Dis. 2011;43 Suppl 1:S32–9.
2. Pinzani M, Rosselli M, Zuckermann M. Liver cirrhosis. Best Pract Res Clin Gastroenterol. 2011;25:281–90.
3. Bonis PAL, Friedman SL, Kaplan MM. Is liver fibrosis reversible? N Engl J Med. 2001;344:452–4.
4. Friedman SL. Cytokines and fibrogenesis. Semin Liver Dis. 1999;19:129–40.
5. Li D, Friedman SL. Liver fibrogenesis and the role of hepatic stellate cells: new insights and prospects for therapy. J Gastroenterol Hepatol. 1999;14:618–33.
6. Lee UE, Friedman SL. Mechanisms of hepatic fibrogenesis. Best Pract Res Clin Gastroenterol. 2011;25:195–206.
7. Coulon S, Heindryckx F, Geerts A, Van Steenkiste C, Colle I, Van Vlierberghe H. Angiogenesis in chronic liver disease and its complications. Liver Int. 2011;31:146–62.

8. Peer D, Karp JM, Hong S, Farokhzad OC, Margalit R, Langer R. Nanocarriers as an emerging platform for cancer therapy. Nat Nanotechnol. 2007;2:751–60.
9. Chen X, Sun R, Hu J, Mo Z, Yang Z, Liao D, *et al.* Attenuation of bleomycin-induced lung fibrosis by oxymatrine is associated with regulation of fibroblast proliferation and collagen production in primary culture. Basic Clin Pharmacol Toxicol. 2008;103:278–86.
10. Zhang Y, Wang S, Li Y, Xiao Z, Hu Z, Zhang J. Sophocarpine and matrine inhibit the production of TNF-alpha and IL-6 in murine macrophages and prevent cachexia-related symptoms induced by colon26 adenocarcinoma in mice. Int Immunopharmacol. 2008;8:1767–72.
11. Wu XL, Hang TJ, Shen JP, Zhang YD. Determination and pharmacokinetic study of oxymatrine and its metabolite matrine in human plasma by liquid chromatography tandem mass spectrometry. J Pharm Biomed Anal. 2006;41:918–24.
12. Daneshpour N, Griffin M, Collighan R, Perrie Y. Targeted delivery of a novel group of site-directed transglutaminase inhibitors to the liver using liposomes: a new approach for the potential treatment of liver fibrosis. J Drug Target. 2010;19:624–31.
13. Wang T, Yin X, Lu Y, Shan W, Xiong S. Formulation, antileukemia mechanism, pharmacokinetics, and biodistribution of a novel liposomal emodin. Int J Nanomedicine. 2012;7:2325–37.
14. Di Sario A, Candelaresi C, Omenetti A, Benedetti A. Vitamin E in chronic liver diseases and liver fibrosis. Vitam Horm. 2007;76:551–73.
15. Liu SL, Degli Esposti S, Yao T, Diehl AM, Zern MA. Vitamin E therapy of acute CCl4-induced hepatic injury in mice is associated with inhibition of nuclear factor kappa B binding. Hepatology. 1995;22:1474–81.
16. von Herbay A, Stahl W, Niederau C, Sies H. Vitamin E improves the aminotransferase status of patients suffering from viral hepatitis C: a randomized, double-blind, placebo-controlled study. Free Radic Res. 1997;27:599–605.
17. Helson L, Helson C. Effects of vitamin E on fibroblast fibronectin. Nutr Cancer. 1985;7:221–7.
18. Latella G, Vetuschi A, Sferra R, Catitti V, D'Angelo A, Zanninelli G, *et al.* Targeted disruption of Smad3 confers resistance to the development of dimethylnitrosamine-induced hepatic fibrosis in mice. Liver Int. 2009;29:997–1009.
19. Nasir GA, Mohsin S, Khan M, Shams S, Ali G, Khan SN, *et al.* Mesenchymal stem cells and Interleukin-6 attenuate liver fibrosis in mice. J Transl Med. 2013;11:78. doi:10.1186/1479-5876-11-78.
20. Chong LW, Hsu YC, Chiu YT, Yang KC, Huang YT. Anti-fibrotic effects of thalidomide on hepatic stellate cells and dimethylnitrosamine-intoxicated rats. J Biomed Sci. 2006;13:403–18.
21. Miao CY, Deng SH, Chen JF. Studies on preparation of anionic oxymatrine liposomes and its physicochemical properties. Chin Pharm J. 2006;41:1400–4.
22. Du S, Deng Y. Studies on the encapsulation of oxymatrine into liposomes by ethanol injection and pH gradient method. Drug Dev Ind Pharm. 2006;32:791–7.
23. Zucker D, Marcus D, Barenholz Y, Goldblum A. Liposome drugs' loading efficiency: a working model based on loading conditions and drug's physicochemical properties. J Control Release. 2009;139:73–80.
24. Haran G, Cohen R, Bar LK, Barenholz Y. Transmembrane ammonium sulfate gradients in liposomes produce efficient and stable entrapment of amphipathic weak bases. Biochim Biophys Acta. 1993;1151:201–15.
25. Xiong S, Li H, Yu B, Wu J, Lee RJ. Triggering liposomal drug release with a lysosomotropic agent. J Pharm Sci. 2010;99:5011–8.
26. Fritze A, Hens F, Kimpfler A, Schubert R, Peschka-Süss R. Remote loading of doxorubicin into liposomes driven by a transmembrane phosphate gradient. Biochim Biophys Acta. 2006;1758:1633–40.
27. Ueno T, Nakamura T, Torimura T, Sata M. Angiogenic cell therapy for hepatic fibrosis. Med Mol Morphol. 2006;39:16–21.
28. Lee CP, Shih PH, Hsu CL, Yen GC. Hepatoprotection of tea seed oil (*Camellia oleifera* Abel.) against CCl_4-induced oxidative damage in rats. Food Chem Toxicol. 2007;45:888–95.
29. Shah AR, Banerjee R. Effect of D-α-tocopheryl polyethylene glycol 1000 succinate (TPGS) on surfactant monolayers. Colloids Surf B: Biointerfaces. 2011;85:116–24.